Flow Control Analysis of S-duct Diffuser Inlet

Lian.Xiaochun Zhang.Lifen Wu.Dingyi
School of Power and Energy, Northwestern Polytechnical University, Shaan'xi 710072

Keywords: AJCPP, Propulsion, S-duct Inlet, Swirl, Flow Control, Vortex Generator

Abstract

An numerical investigation of the flow characteristics inside a diffusing S-duct inlet with and without vortex generators (VGs) was conducted. The primary discussion herein focuses on development of secondary flow in the S-duct with and without VGs, pressure recovery and distortion at the exit are also discussed. Full three-dimensional Navier-Stokes equations are solved using finite volume method and $k-\varepsilon$ turbulence model is employed. In order to validate the credibility of the numerical methods, predicted results of surface pressure are compared with flight test for the S-duct inlet without VGs, and it shows fairly good agreement. The result shows that VGs alter the flow characteristics in the S-duct and are effective in reducing distortion and ineffective in improving pressure recovery.

Introduction

Since the mid-1980s, S-duct inlets have been the object of a strong interest in aircraft. The high degrees of centerline curvature and large changes in cross-sectional area give rise to secondary flow and boundary layer separation which will significantly reduce engine performance. So it's necessary to take measures to control flow in S-duct inlet.

The objective of this research is to investigate detailed flow characteristics in an S-duct inlet and find ways to reduce distortion. Many computational and experimental work have been done[1~6], usually a S-duct model was used. In this paper, the S-duct inlet is a real inlet, also airframe and boundary layer diverter are taken into account. To better observed development of secondary flow in the diffusing S-duct inlet, CFD computations are performed and S-duct inlets with VGs in two different locations are also predicted.

Computation

The geometry of the S-duct inlet contains diffusing S-duct, airframe and boundary layer diverter. The S-duct has a cross-sectional area change going from a retangular at the entrance to a full circle at the exit. At the entrance, there have three control planes. The first is fixed, the second and third are movable. Incoming flow was undisturbed, so a enough large square, 50m $\times$50m$\times$50m, was selected as outer flow's computational domain. Because of attack angle and sideslip angle being zero, half of the computational domain was applied as shown in Fig.1.

The boundary conditions were static pressure, Mach number and temperature specified at pressure far field, no slip at the walls, static pressure specified at the exit of the S-duct inlet and outer flow, and symmetry about the xz-plane. All reported tests were conducted with incoming flow Mach number of 1.4, flight altitude of 11000m. Commercial software GAMBIT was used to generate unstructured grids. The total number of grids was about 0.6 million. Full three-dimensional Reynolds-averaged Navier-Stokes equations in strong conservation form were solved using commercial software FLUENT. Standard $k-\varepsilon$ turbulence model and wall function were used in near wall treatment.

To get better performance of the S-duct inlet, VGs were used in this research. The cross-section of the VG is elliptic, and the height is 20mm. Angle between vortex generators and incoming flow is 10° as shown in Fig.2.

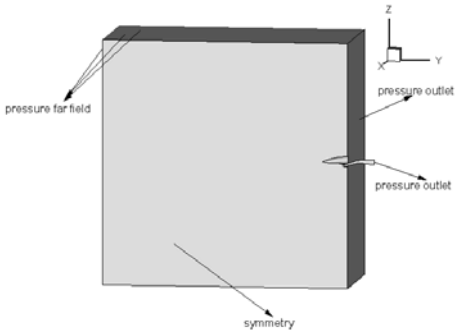

Fig.1 Computational domain and boundary condition

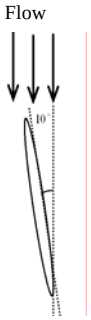

Fig.2 Setting angle of VG

Validation

To validate the credibility of the computational method used in this paper, static pressure for some discrete points on bottom and side of the S-duct surface without VGs was compared with flight test data. Fig.3 is the locations of compared discrete points, and Fig.4 is the results of comparison. It shows good agreement between prediction and flight test. And it indicates the numerical method used here is reasonable.

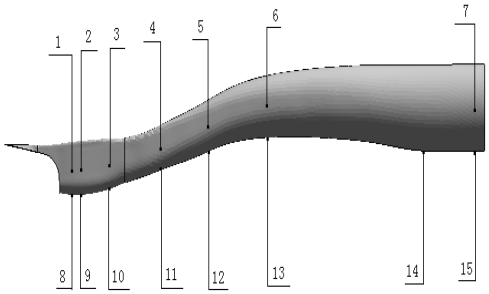

Fig.3 Location of measured points

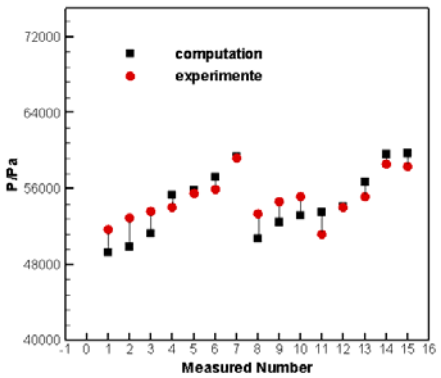

Fig.4 CFD/Experiment pressure comparisons

Results and Discussion

Flow in and outside S-duct without VGs was analyzed firstly. Fig.5 shows Mach number contour in symmetry plane. Around airframe head, there was a conical shock wave, flow was decelerated but still supersonic speed. On the top lip, a shock wave is legible which is fexlilable than the first. After this shock wave, airflow was subsonic speed, and flow into S-duct inlet.

To better observe flow in the S-duct inlet, total pressure recovery and secondary flow in six cross-stream planes of the S-duct without VGs is presented in fig.6 and fig.7. The development of secondary flow in the S-duct inlet without VGs were revealed in Fig.6. In the first bend, due to the duct's curvature, a centrifugal force is produced, and pressure of outside bend is higher than inside bend, so a pressure gradient is induced in cross-stream plane1 and 2. In order to banlance the centrifugal force, fluid has a trend to be pushed to the inside of the duct, so that the direction of the secondary flow is upward. Boundary layer in two-sides was swept to the top more readily than the core flow as shown in plane3. After second bend (as shown in plane4 to 6), a pair of counter-rotating vortices were formed. As flow progressed downstream, it became larger and clearer. Secondary flow affects pressure recovery as shown in fig7. In plane 1, low momentum fluid concentrate on the top of the duct. As the flow progressed downstream, low momentum fluid developed from top to the centre of the duct. This because secondary flow is upward before the second bend, low momentum fluid was swept along side wall to the top of the duct by secondary flow, so fluid already on the top was pushed to the center of the duct. In the second bend, the direction of the secondary flow reversed. The top boundary layer is thickest, secondary flow reversal should firstly occur here, so that a pair of counter-rotating vortices came into being. The vortices continually convected the low momentum fluid towards the center of the duct. The convection degraded performance of the duct.

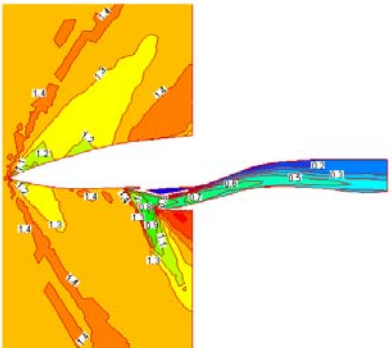

Fig.5 Mach number in symmetry plane

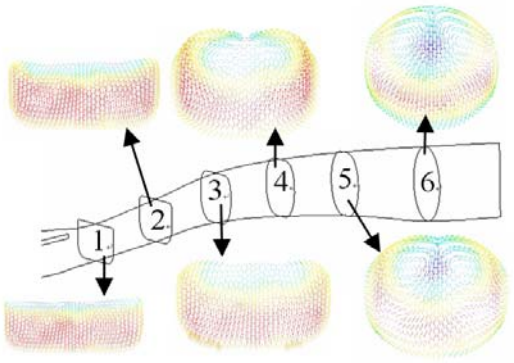

Fig.6 Secondary flow in six cross-stream planes in S-duct without VGs

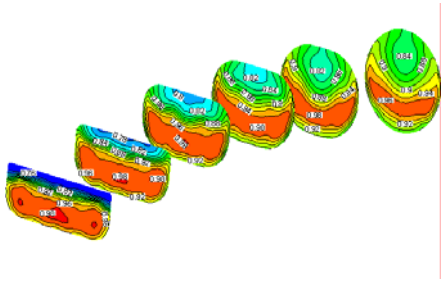

Fig.7 Total pressure recovery in six cross-stream planes

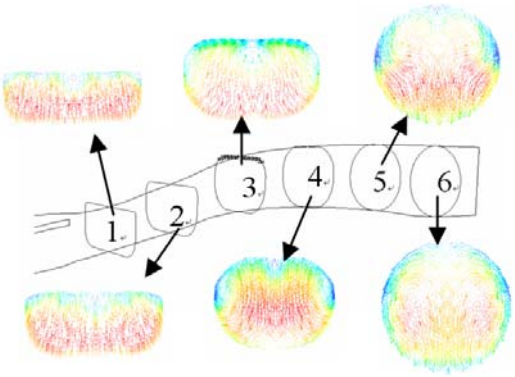

Fig.8 Secondary flow in six cross-stream planes in S-duct with VGs1

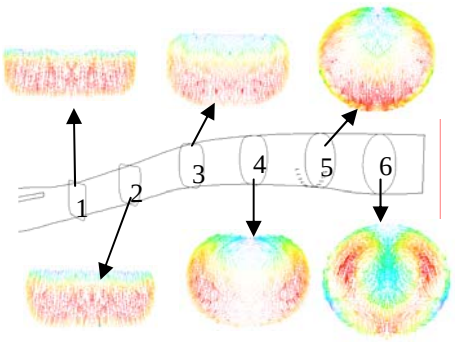

Fig.9 Secondary flow in six cross-stream planes in S-duct with VGs2

Fig.8-Fig.9 exhibit the development of secondary flow in the S-duct inlet with VGs at two different location. At location 1, VGs were located on the top of the duct before second bend; at location 2, VGs were on the bottom of the duct after second bend. In fig.8, two vortices revolving reversal were produced in plane 3. Due to the VGs, boundary layer can't be pushed to the top of the duct by secondary flow, but core flow were continuously swept to the top, so two sides boundary layer was extruded and forced to change direction forming a pair of vortices. As flow progressed downstream, it became larger but its intensity was weakened.

In fig.9, development of secondary flow in plane1 to 4 were similar to the secondary flow in fig.7, from plane 5, it has some difference. At the bottom of plane 5, there were some small vortices resulting from VGs. As the flow developed and duct curvature changed, these small vortices became a pair of reversal revolving vortices.

Table 1 performance comparison at exit plane

	σ_{av}	$\Delta\sigma_0$	*DC*(60)	*SC*(60)
Bare S-duct	0.90797	0.02743	0.0338	0.0277
Location 1	0.90807	0.02433	0.0301	0.0211
Location 2	0.90876	0.02314	0.0288	0.0177

Performance of the diffusing S-duct inlet with and without VGs was compared to each other in table 1. Though the comparison, it shows that installation of VGs in the S-duct inlet at two different locations helped to decrease distortion and swirl, but it was ineffective to increase the pressure recovery.

Conclusion

Development of secondary flow in the S-duct with and without VGs was carefully discussed. For the S-duct without VGs, counter-rotating vortices were formed after second bend. Installation of VGs changed the development of secondary flow and decreased the distortion and swirl of the S-duct, but it was ineffective in improving pressure recovery.

References

1) Sullerey, R. K., Mangat, V. S., Padhi, A., Flow control in serpentine inlet using vortex generator jets, AIAA 2006-3499.
2) Jirásek, A, Development and application of design strategy for design of vortex generator flow control in inlets, AIAA 2006-1050.
3) Tournier, S. E., Paduano, J. D., Flow analysis and control in a transonic inlet. AIAA-2005-4734.
4) Mohler, S. R., WIND-US flow calculations for the M2129 S-duct using structured and unstructured grids, AIAA-2004-0525.
5) Anabtawi, A. J., Blackwelder, R. F, Lissaman, P. B. S., Liebeck, R. H., An experimental study of vortex generators in boundary layer ingesting diffusers with a centerline offset, AIAA 99-2110.
6) Harloff, G. J., Reichert, B. A., Wellborn, S. R., Navier-stokes analysis and experimental data comparison of compressible flow in a diffusing S-duct. AIAA-92-2699.